Ab initio calculation of dc resistivity in liquid Al, Na and Pb

2007 J. Phys.: Condens. Matter 19 196105

(http://iopscience.iop.org/0953-8984/19/19/196105)

IOP PUBLISHING JOURNAL OF PHYSICS: CONDENSED MATTER

J. Phys.: Condens. Matter **19** (2007) 196105 (12pp) doi:10.1088/0953-8984/19/19/196105

Ab initio calculation of dc resistivity in liquid Al, Na and Pb

F Knider, J Hugel and A V Postnikov

Laboratoire de Physique des Milieux Denses, Institut de Physique électronique et Chimie, Paul Verlaine Université–Metz, 1 Boulevard Arago, F-57078, Metz Cedex 3, France

E-mail: postnikov@univ-metz.fr

Received 9 February 2007, in final form 2 April 2007
Published 20 April 2007
Online at stacks.iop.org/JPhysCM/19/196105

Abstract

The dc conductivities of Al, Na and Pb in their liquid phase just above the melting point are calculated from first principles on the basis of density functional theory. We use the SIESTA code, molecular dynamics simulations with a Nosé thermostat to generate representative structural snapshots in the liquid and Kubo–Greenwood formalism to calculate the optical conductivity. The dc conductivity comes from averaging the latter property over a number of structures and extrapolating to zero frequency. The calculated values fall within 1% of experimental data. A correction to the dipole matrix elements calculated via the momentum operator, due to non-locality of the pseudopotential, is very important for Na (where it increases the dc conductivity by about 75% to meet the experimental value), much smaller for Al and practically negligible for Pb.

(Some figures in this article are in colour only in the electronic version)

1. Introduction

The electrical resistivity in condensed media is often influenced by the presence of scattering mechanisms which are difficult to specify and grasp in a first principles calculation. When discussing metals, the mobility of nearly free electrons at the Fermi surface yield an important contribution to conductivity, which is further shaped by interband electronic excitations (optical transitions). In the ideal case, the dc conductivity is directly related to the imaginary part of the dielectric function, taken at its $\omega \to 0$ limit, and the dielectric function is readily available from the electronic band structure via the Kubo–Greenwood formalism (Kubo 1957, Greenwood 1958). There are several limiting cases where this approach has proven to work well. One is for ideally perfect pure metals at low temperatures, where the presence of scattering mechanisms in crystal other than purely electronic excitations can be neglected. The opposite limit is a case of liquid, or gaseous, metal, where the structural disorder affects the electronic scattering so strongly that it becomes the dominant scattering mechanism, permitting us to neglect

possible influence of phonons or external defects. A number of successful calculations so far done (Desjarlais *et al* 2002, Recoules *et al* 2003, Recoules and Crocombette 2005, Alemany *et al* 2004) indicate that the higher the temperature the better the quality of a first-principles prediction. This conveniently contrasts with the phenomenological Ziman's approach (Ziman 1961b, 1961a), which depends on knowing the liquid structure factor.

The practical problem in performing *ab initio* calculations of conductivity in liquid metals shifts toward dynamical and statistical components, i.e. a need to consider a large enough simulation cell to allow a fair simulation of structural disorder in liquid and a long enough molecular dynamics (MD) history to equilibrate the system and perform the averaging of results over sufficient numbers of structural 'snapshots'. Large numbers of atoms, large numbers of simulation steps and the lack of symmetry leave few calculation methods which are able to cope with the problem in practice. Previous applications mostly used plane wave codes (Silvestrelli *et al* 1997, Recoules *et al* 2003, Desjarlais *et al* 2002).

In the present work, we discuss the use of the SIESTA method (Ordejón *et al* 1996, Soler *et al* 2002), with its atom-centred basis set of localized numerical functions. As a not yet so common application of this particular method to the problem in question, it raises a number of specific issues of verification of approach, optimal choice of simulation parameters etc. We discuss these issues for three elemental metals, one of which (Al) is quite well studied, another one (Na) is, according to previous experience, somehow problematic, and for the third one (Pb) we are not aware of any previous *ab initio* calculations of conductivity.

The paper is organized as follows: section 2 briefly overviews the theory, section 3 gives details of SIESTA calculation, section 4 outlines the results.

2. Theoretical model

The optical conductivity $\sigma(\omega)$ is expressed through the imaginary part ε_2 of the dielectric function $\varepsilon(\omega, \mathbf{q})$ as:

$$\sigma(\omega) = \varepsilon_0\, \omega \varepsilon_2(\omega, \mathbf{q}{\to}0). \tag{1}$$

The widely used formula for $\varepsilon(\omega, \mathbf{q})$ (see, e.g. Maksimov *et al* 1988) is

$$\varepsilon(\omega, \mathbf{q}) = 1 + \frac{8\pi e^2}{\Omega \mathbf{q}^2} \sum_{\mathbf{k},n,m} \frac{\left|\langle \mathbf{k}+\mathbf{q}, n|\mathrm{e}^{\mathrm{i}\mathbf{q}\mathbf{r}}|\mathbf{k}, m\rangle\right|^2 \left(f_{\mathbf{k},m} - f_{\mathbf{k}+\mathbf{q},n}\right)}{E_{\mathbf{k},m} - E_{\mathbf{k}+\mathbf{q},n} + \hbar\omega + \mathrm{i}\delta}, \tag{2}$$

where band energies $E_{\mathbf{k},n}$, entering the Fermi distribution function $f_{\mathbf{k},n}$, and Kohn–Sham eigenfunctions $|\mathbf{k}, n\rangle$ may follow from a band structure calculation within the density functional theory (DFT). For metals, an accepted routine is (see, e.g. Ehrenreich and Philipp 1962) to split the dielectric function, taken in the $\mathbf{q} \to 0$ limit, into the intraband contribution, which is cast in the form known from the Drude free electron theory (Schulz 1957), and the interband contribution. These two make respectively the first and the second line in the following formula:

$$\begin{aligned}\varepsilon(\omega) = 1 &- \frac{\omega_\mathrm{p}^2}{\omega(\omega + \mathrm{i}/\tau)} \\ &+ \frac{8\pi e^2\hbar^2}{3m^2(2\pi)^3} \int \mathrm{d}\mathbf{k} \sum_{n\neq m} \frac{2 f_{\mathbf{k},n}(1 - f_{\mathbf{k},m})\, |\langle \mathbf{k}, n|\mathbf{p}|\mathbf{k}, m\rangle|^2}{(E_{\mathbf{k}m} - E_{\mathbf{k}n})[(E_{\mathbf{k}m} - E_{\mathbf{k}n})^2 - (\hbar\omega)^2 + \mathrm{i}\delta]},\end{aligned} \tag{3}$$

where one of several equivalent expressions for the dipole matrix element, in terms of the momentum operator, is chosen—see, e.g. Uspenski *et al* (1983) for comparing the accuracy of alternative expressions in practical calculations. The generalization of the optical conductivity

tensor for the relativistic case, with appropriately chosen dipole matrix elements but otherwise a similar separation of the general formula into intraband and interband contributions, is given by Antonov *et al* (1999). In the Drude free electron theory, the conductivity (1) due to the intraband term falls down from its maximum at $\omega = 0$ as a Lorentzian function, governed by two parameters, the plasma frequency ω_p and relaxation time τ:

$$\sigma^D = \frac{\omega_p^2/\tau}{\omega^2 + 1/\tau^2}. \tag{4}$$

When the *ab initio* results for the full dielectric function (2) are cast, with regard to their intraband part, into the Drude form, both parameters can follow from the calculation. In particular, the plasma frequency is related to the Fermi velocity, integrated over the Fermi surface

$$\omega_p^2 = \frac{8\pi e^2}{3\Omega} \sum_{\mathbf{k},n} \left| \frac{1}{\hbar} \frac{\partial E_{\mathbf{k},n}}{\partial \mathbf{k}} \right|^2 \delta(E_{\mathbf{k},n} - E_F). \tag{5}$$

A way to calculate intraband relaxation time τ has been outlined by Mazin *et al* (1984). However, in the calculations done for liquid metals—that is, using large unit cells with quite 'chaotic' distribution of atoms, a choice of τ as an external (coming from experiment) or an internal but adjustable parameter, would often suffice, for the following reason. In perfect metals, the intraband contribution to conductivity dominates at low frequencies, because the interband optical absorption, and hence related contributions to the electronic conductivity, start at the energies of an order of 10^{-1}–10^{0} eV (see a discussion on crystalline Al below). In a simulation for a liquid, however, when a large enough simulation cell with many atoms and a fair amount of disorder is taken, the soup of electron energy bands within a reduced Brillouin zone creates many interband transitions, which may start already at arbitrarily low energies. Therefore the intraband contribution would often get lost beneath a much larger interband part, even in the limit of low frequencies. The evaluation of dc conductivity becomes, therefore, an issue of accurate extrapolation to $\omega = 0$. In some works the Drude analytical form (4) was considered as a natural extrapolation function for the total frequency-dependent conductivity and the τ value was extracted from this fit. We performed our conductivity calculations in a twofold manner. As a first try, we allowed the summation over all transitions, a follow-up for the conductivity (1) from the general formula (2), without a separation into intraband and interband terms. For practical reasons, we allowed a broadening parameter $\delta = 0.2$ eV, to suppress divergences. In this approach, however, we applied a straightforward formula for the calculation of the dipole matrix element (with a gradient operator), which in fact needs to be corrected when used in combination with non-local pseudopotentials V_{nl}, because of the following. As was outlined by e.g. Baroni and Resta (1986), the approximation for the dipole matrix elements in (2), taken in the limit of $\mathbf{q} \to 0$, is formally that of the position operator (times i$\mathbf{q}$), but for practical reasons, in a system with periodic boundary conditions, it is conveniently expressed via the momentum operator:

$$\begin{aligned}\langle \mathbf{k}+\mathbf{q}, n|e^{i\mathbf{qr}}|\mathbf{k}, m\rangle \simeq i\mathbf{q}\langle \mathbf{k}, n|\,\mathbf{r}\,|\mathbf{k}, m\rangle &= \frac{i\mathbf{q}}{E_{\mathbf{k},m} - E_{\mathbf{k},n}} \langle \mathbf{k}, n|\,[\mathcal{H}, \mathbf{r}]\,|\mathbf{k}, m\rangle \\ &= \frac{\mathbf{q}}{\omega_{mn}} \langle \mathbf{k}, n| \left(\frac{\mathbf{p}}{m} + \frac{i}{\hbar}\,[V_{nl}, \mathbf{r}] \right) |\mathbf{k}, m\rangle. \end{aligned} \tag{6}$$

The correction due to the commutator $[V_{nl}, \mathbf{r}]$ does not appear in all-electron calculations, but has to be accounted for in calculations which employ non-local pseudopotentials. A discussion on some tests for the size of this non-local correction has been offered by Read and Needs (1991). Recoules *et al* (2003) emphasized the importance of non-local corrections

with respect to their calculations for an Al plasma, whereas Silvestrelli *et al* (1997) calculated the conductivity of liquid sodium without correcting the matrix elements.

An option to calculate dielectric function in the SIESTA code, implemented by Sánchez-Portal, takes the non-local correction into account. This feature, now a standard option in SIESTA, introduces a splitting into intraband and interband parts according to equation (3), with the plasma frequency ω_p being evaluated along equation (5), but the relaxation time τ remaining an external parameter. This was our second calculation ansatz, numerically superior to the first one but containing certain impureness, in a strict *'ab initio'* sense. We refer to these two calculation approaches as 'uncorrected' and 'corrected', when comparing their results in section 4.

The calculation task as such splits into the evaluation of conductivity along the above formulae, and the MD part, yielding a sequence of atomic configurations, for which the Kubo–Greenwood analysis is applied. The MD is driven by calculated forces, which include in SIESTA the Hellmann–Feynman terms with Pulay corrections.

The effect of the imposed temperature is twofold. First, there is an electronic temperature, whose effect is a smearing of the Fermi function, that amounts, however, to merely 0.086 eV for 1000 K. More importantly, the atom dynamics is influenced by the temperature via coupling to the Nosé thermostat (Nosé 1991). The temperature set by the thermostat has a major effect on the resulting snapshots of the atomic distribution in those MD steps which have been selected to perform the evaluation of the dielectric function and to take an average.

3. Computational details

The solution of the electronic structure problem in each step of the MD simulation, evaluation of the forces on atoms into the next MD step and imposing the coupling to the thermostat is all organized within the SIESTA code (Ordejón *et al* 1996, Soler *et al* 2002). This code relies on norm-conserving pseudopotentials, which have been constructed along the Troullier–Martins scheme (Troullier and Martins 1991), using the valence atomic configurations and pseudization radii as follows (the radii are set in brackets, in bohr units, for each l-channel): Na $3s^1(2.95)3p^0(3.50)3d^0(2.95)4f^0(2.95)$; Al $3s^2(2.60)3p^1(2.80)3d^0(2.30)4f^0(2.30)$; Pb $6s^2(2.00)6p^1(2.00)5d^{10}(2.00)5f^0(1.50)$. The pseudopotential setting for Na was as recommended by Junquera (along with the basis setting, see below) and uploaded at the SIESTA web page[1]. The results of the original tests for this pseudopotential are provided by Junquera *et al* (2001). With respect to the construction of the basis set, sodium demands the most care among the three elements we studied. For Al and Pb, the 'standard' basis set of the double-ζ plus polarization orbitals (DZP) quality provides a good enough band structure well beyond the Fermi level (see the figures and discussion in subsequent sections) to yield a faithful description of optical excitations in the energy interval of interest. With the energy shift parameter (that controlling the spatial confinements of pseudoatomic orbitals, used as basis functions) of 0.02 Ryd, the maximal extension of Al basis functions is 7.1 bohr, whereas the nearest-neighbour distance in the solid phase is 5.41 bohr, yielding a sufficient overlap to reproduce a good energy band structure. The situation for Pb is similar. But for sodium, which has very low density and an interatomic distance of about 7.0 bohr in the solid phase, the basis functions constructed with the above energy shift parameter will not overlap at all. The lowering of the energy shift parameter leads to more diffuse basis functions, but at too slow a pace to yield a technically satisfactory solution. Another way was pursued by Junquera *et al* (2001) who tailored the Na basis set with the soft confinement radii of 6.43 bohr in the 3s-channel and 6.10 bohr in the 3p-channel. With the double-ζ quality for the s states

[1] http://www.uam.es/siesta

Table 1. Densities, temperatures and relaxation times.

Liquid metal	Density (g cm^{-3})	Melting T (K)	Simulation T (K)	τ (10^{-16} s)
Al	2.35	933.48	1000	6.7[a]
Na	0.93	370.90	400	70[b]
Pb	10.31	600.62	650	3.26[c]

[a] Recoules *et al* (2002).
[b] Silvestrelli *et al* (1997).
[c] El Ghemmaz (1996).

and single-ζ quality for the p states (five functions per atom, in total), the equilibrium elastic and cohesion properties for Na come out in good agreement with plane wave and all-electron calculations (all of them somehow deviating from experiment, though), as can be seen from table 4 of Junquera *et al* (2001).

We tested the effect of enhancing the basis up to triple-ζ in both s and p channels and observed big changes at energies at about 15 eV above the Fermi level, but no visible changes (and also fair agreement with all-electron results) within 5 eV into the empty states, which covers the range of interest in our calculations of optical conductivity.

In terms of practically performing the calculations, we tried to optimize the amount of work related with the need to: (i) treat many atoms per cell, for a reasonable simulation of liquid; (ii) use sufficiently dense **k**-mesh for good evaluation of forces in the MD and especially for the calculation of optical conductivity; (iii) allow long enough history of MD for the equilibration of system and for averaging the conductivity results over a sufficient number of configurations. Our choice amounted to 32 atoms in the cell, $8 \times 8 \times 8$ divisions of the Brillouin zone in a regular electronic structure calculation, and $12 \times 12 \times 12$ divisions in the calculation of optical conductivity; not less than $\sim 10^3$ steps of MD after the equilibration, with averaging of $\sigma(\omega)$ over $\sim$20 evenly distributed sample steps.

The values of dc conductivity were extracted from extrapolating the calculated $\sigma(\omega)$ function to $\omega = 0$. In the calculation along our second scheme (corrected dipole matrix elements; separation of conductivity into interband and Drude parts), the plasma frequency is calculated in SIESTA according to equation (5) and the relaxation time τ remains the only empirical parameter in our calculation. Its values have been extracted from the literature and summarized, for the three elements, in table 1.

4. Results and discussion

4.1. Solid aluminium

Before studying the liquid phases for aluminium, sodium and lead, we consider a benchmark case of perfect solid aluminium, in its cubic face centred phase with a lattice parameter of 7.62 bohr. The density of states (DOS), calculated for the 4-atom cubic cell with $18 \times 18 \times 18$ k-space divisions in the Brillouin zone, is shown in figure 1(a). It rather faithfully reproduces the known deviations from the free-electron parabola below and above the Fermi level. The optical conductivity of Al has been measured by Bos and Lynch (1970) and calculated from first principles by Alouani *et al* (1986) which revealed a peak in $\varepsilon_2(\omega)$ near $\sim$1.5 eV, also present in our calculation. In fact, the optical conductivity curve (figure 1(b)) shows two structures at 0.48 and 1.6 eV, which are in close agreement with the theoretical results of Tups and Syassen (1984). However, the interband structure at 0.48 eV does not appear in the experimental spectrum because it is wiped out by the large Drude contribution.

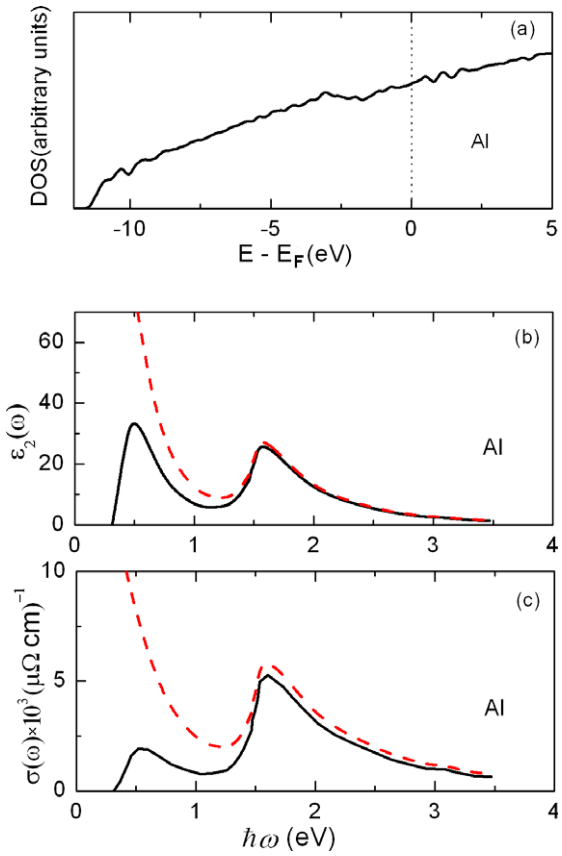

Figure 1. Electronic structure calculation results for fcc Al ($a = 7.62$ au), with the temperature smearing corresponding to 300 K. (a) Density of states; (b) imaginary part of the dielectric function, interband contribution (solid line) and total (dashed line); (c) optical conductivity, interband (solid line) and total (dashed line).

4.2. Liquid phase results

The three metals are simulated within a cubic cell whose size is proportional to the selected number of atoms (32; also 64 for Al) and whose dimension is deduced from the experimental density near the melting point. The densities with their corresponding temperatures are given in table 1.

To confirm that the quantum molecular simulation converged towards thermal equilibrium, the pair correlation functions have been calculated for the three metals and are shown in figure 2. The theoretical curves do not perfectly match the experimental ones, owing to our limited supercell size, but otherwise the positions and relative intensities of peaks are fairly well reproduced. We note that earlier calculation results for this property are available from Silvestrelli *et al* (1997) (Na, 90 atoms in periodic cell), Kresse and Hafner (1993) (Na, 54 atoms), Recoules and Crocombette (2005) (Al, 108 atoms), Alemany *et al* (2004) (Al, 205 atoms). The experimental radial density function for liquid lead is reported by Kaplow *et al* (1965) who, however, set the first peak too close in comparison to later experimental findings by Waseda (1980) and our calculations.

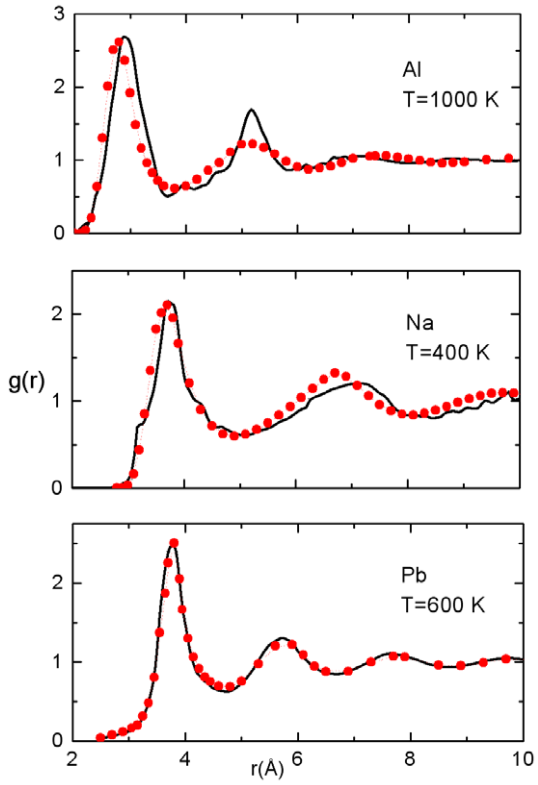

Figure 2. Calculated pair correlation functions for liquid metals Al, Na and Pb close to their melting points (solid lines) in comparison with experimental data (full circles) from Waseda (1980).

4.3. Density of states

The liquid aluminium DOS in figure 3(a), coming from 3s and 3p conduction electrons, looks like that of the solid metal. The fact that the densities of states in liquid and solid Al exhibit the overall same shape is well known (Recoules and Crocombette 2005). We compare the results obtained with different simulation sizes, of 32 and 64 atoms (as snapshots after independent sequences of MD simulation) and conclude that they are indistinguishable for any practical purposes.

For sodium two DOS, both for a 32 atom cell, have been depicted in figure 3(b), one related to the tuned basis of (five in total) 3s and 3p functions as discussed above, and another one with three 3s-type basis functions only. The more limited basis shows a rapid disappearance of electronic states above the Fermi level, which may be acceptable for ground-state results and MD trajectories, but considerably deteriorates optical properties.

The DOS of lead is spanned by the 6s, 6p and 5d orbitals and is shown in figure 3(c). It reveals the gap in the occupied states of about 1.5 eV. A similar DOS shape, with a gap of about 1.4 eV, has been reported by Jank and Hafner (1990). Both results are in agreement the experimental measurements of Indlekofer, as cited by Ben Abdellah *et al* (2003).

4.4. Optical conductivity

The computed optical conductivities $\sigma(\omega)$ are drawn in figure 4. For each metal, two similar spectra have been reproduced for a 32 atom supercell. The curves A correspond to a calculation

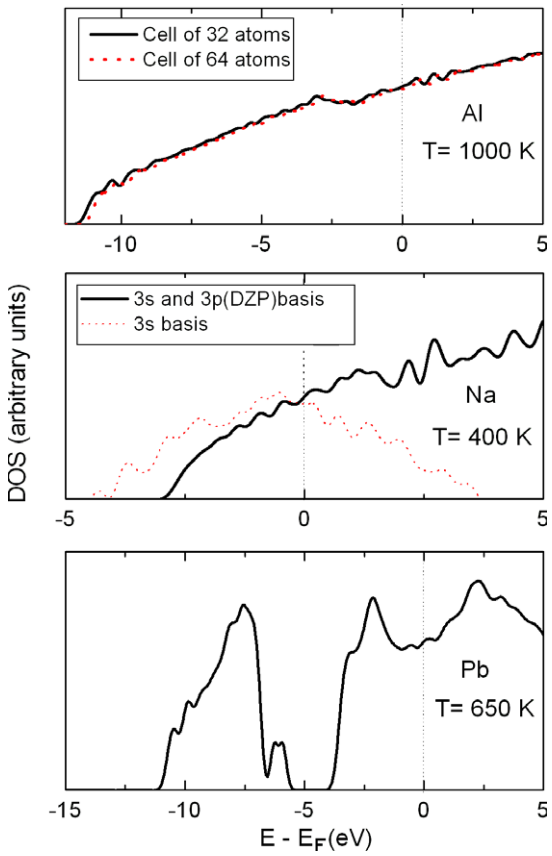

Figure 3. Density of states of liquid Al, Na and Pb. Zero energy marks the Fermi level. For aluminium, the results obtained with two different simulation cell sizes are shown, and for Na—for two different basis sets. See text for details.

of interband conductivity as in the second line of equation (3), with dipole matrix elements corrected for the non-local pseudopotential according to equation (6) and the Drude term specifically added. The curves B correspond to a straightforward evaluation of the momentum matrix element, without correction, and summation over all states, in the spirit of equation (2). One can observe that the correction in all cases enhances the conductivity; otherwise the A and B results are in fair agreement for aluminium and lead, but markedly off for sodium. An analysis of non-local correction over several atoms carried out by Read and Needs (1991) indicates that its effect is largest for, say, s–p transition when the corresponding components of pseudopotential markedly differ in their depth, as is the case for $l = 0$ and 1 of carbon. One can easily see[2] that the corresponding difference is in fact much more pronounced for sodium, with the $l = 0$ component of pseudopotential being markedly repulsive within a large region around the core, and the $l = 1$ component being moderately attractive. Such marked difference in the pseudopotential components is not at all typical for Al and Pb whose l-channels of pseudopotential remain moderately attractive (even if $l = 1$ for Al is quite shallow). This observation explains well the singular character of Na among our systems, with regard to the

[2] using, e.g. http://www.tddft.org/programs/octopus/pseudo.php

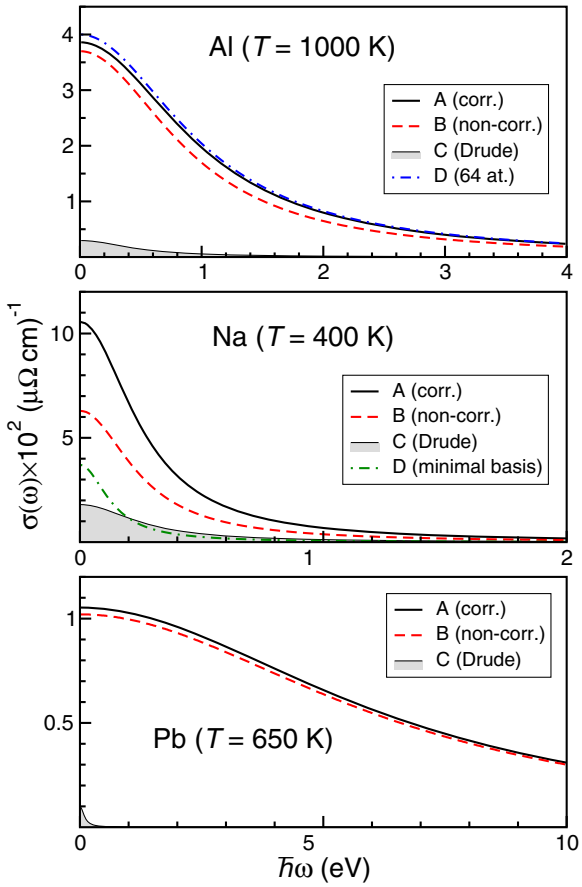

Figure 4. Calculated optical conductivities versus frequency for liquid Al, Na and Pb. The A and B spectra are calculated for a supercell of 32 atoms with, respectively, corrected and non-corrected non-local pseudopotentials; see section 3 for details. The C curve represents the Drude contribution (4) to the (corrected) total conductivity, given by curve A. For aluminium (the top panel), the additional D curve corresponds to a supercell of 64 atoms with a corrected non-local pseudopotential. For sodium (middle panel), the additional D curve corresponds to a reduced basis size, similarly to figure 3.

importance of non-local correction; it shifts the calculated dc conductivity upwards by 75%, thus allowing us to find agreement with the experimental value. A lack of correction may explain the large deviation from experiment in the calculation by Silvestrelli *et al* (1997) (a too high resistivity value). For aluminium, the correction accounts for an increase of about 8% in the calculated dc conductivity, bringing it exactly within the margin of measured values (see the numbers below). For lead, the difference between A and B curves (at $\omega = 0$) amounts to merely 1.6%, hinting at the practical unimportance of the non-local correction for this metal.

We return to the discussion of figure 4. In order to illustrate the relative importance of intraband and interband contributions, we show the Drude part of the optical conductivity (curves C) for each metal, calculated along equation (4) with the values of τ listed in table 1. As could be expected from the respective τ^{-1} values, both the height and the width of the Drude peak are largest in sodium. Moreover, for Al we add a curve D corresponding to a separate MD calculation performed with a larger, 64 atom supercell. Its $\omega \to 0$ extrapolated

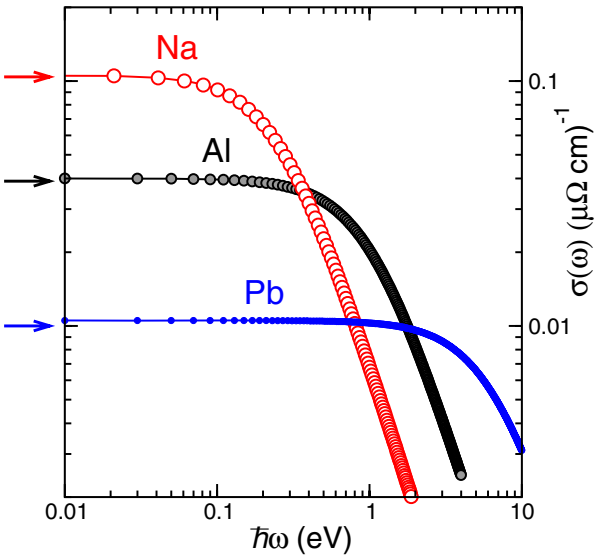

Figure 5. Calculated corrected optical conductivities for a 32 atom unit cell of all three metals. Experimental values are indicated by arrows.

dc conductivity result yields a 2.5% lower value—apparently even closer to the measured one. Still the result falls quite close to that for the 32 atom supercell, hinting that this (admittedly moderate) simulation cell size is not *a priori* too small to result in a meaningful numerical estimate.

For Na, we also add another curve, D, which illustrates the effect of reducing the basis set to include the 3s states only (with non-local correction). One observes a drastic reduction of the optical conductivity, whose limit at zero frequency corresponds to a resistivity about three times larger than the experimental value.

The conductivity curves for all three metals, calculated with non-local correction and for 32 atom cells, are shown in figure 5. One can see the similar functional form, revealing the Lorentzian shape, for all three curves. The logarithmic scale makes the extrapolation to zero frequency particularly easy. A comparison with experimental values (indicated by arrows) is very satisfactory, taking into account the fact that the values for Na and Pb differ by an order of magnitude.

The electrical resistivity is the reverse of optical conductivity at zero frequency, $\sigma_0 = \sigma(\omega \to 0)$. A comparison between calculated and experimental resistivity values is presented in table 2. As can be observed, with care taken about all the issues discussed above, the Kubo–Greenwood *ab initio* formalism successfully describes the electrical resistivity of all three metals in their liquid phase.

5. Conclusion

Whereas the *ab initio* approach to the conductivity of liquid metals, based on dynamic simulations and the Kubo–Greenwood formalism, is not particularly new and has been earlier often used in combination with plane wave pseudopotential calculations, its realization within a computer code like SIESTA, with its compact basis of spatially constrained functions, might bring about certain advantages in terms of computational efficiency. At the same time, however,

Table 2. Theoretical electrical resistivities (in $\mu\Omega$ cm) obtained with parameters given in table 1, in comparison with experimental values.

		Ab initio	
Liquid metal	Experiment	Uncorrected	Corrected
Al	29.20[a]; 24[b]; 28.88[c]	27.72	25.45
Na	9.6[b,d]	16.65	9.52
Pb	95[b]; 97.94[e]	100.04	98.42

[a]Roll and Motz (1957).
[b]Faber (1972), table 5.2. in p. 326.
[c]Ben Abdellah *et al* (2005).
[d]Ashcroft and Lekner (1966).
[e]Ben Abdellah *et al* (2003).

it demands special care in its practical use. In addition to problems shared with the plane wave methods, such as optimal (i.e. sufficiently large to obtain reasonable results and yet conveniently treatable) choice of simulation cell, the duration of MD simulations and the importance of non-local corrections to dipole matrix elements, there are other problems specific to localized basis schemes—first of all, a careful choice of basis extension and size has to be made. In respect of our calculations for three elemental metals, all of which resulted in quite accurate estimations of the experimentally measured resistivities, we can note that the case of lead, a potentially problematic one for the plane wave treatment, turned out to be the most straightforward for the SIESTA calculation. On the other hand, the most typical nearly-free-electron metals, sodium and aluminium, which are expectedly easy for a plane wave calculation, presented certain difficulties in the appropriate choice of basis; these problems, however, could have been successfully overcome. In the course of our work, we also observed that sodium turned out to be very sensitive to the proper inclusion of non-local corrections in the evaluation of dipole matrix elements. We expect that the method of calculating the conductivity of liquid metals with SIESTA is not only complementary to plane wave approaches, but is in fact more advantageous and efficient with respect to certain applications, such as those involving deep semicore states, magnetism or strong electronic correlations.

Acknowledgments

The authors are grateful to J G Gasser for many illuminating discussions on the conductivity of liquid metals, to I I Mazin for the introduction to the basics of optics calculations, to D Sánchez-Portal for the development of the optics calculation part in SIESTA and to J Junquera for the tuning of Na pseudopotential and basis functions in SIESTA.

References

Alemany M M G, Gallego L J and González D J 2004 *Phys. Rev.* B **70** 134206
Alouani M, Koch J M and Khan M A 1986 *J. Phys. F: Met. Phys.* **16** 473–82
Antonov V N, Yaresko A N, Perlov A Y, Nemoshkalenko V V, Oppeneer P M and Eschrig H 1999 *Low Temp. Phys.* **25** 387–406
Ashcroft N W and Lekner J 1966 *Phys. Rev.* **145** 83–90
Baroni S and Resta R 1986 *Phys. Rev.* B **33** 7017–21
Ben Abdellah A, Gasser J G and Grosdidier B 2005 *Phil. Mag.* **85** 1949–66
Ben Abdellah A, Gasser J G, Makradi A, Grosdidier B and Hugel J 2003 *Phys. Rev.* B **68** 184201
Bos L W and Lynch D W 1970 *Phys. Rev. Lett.* **25** 156–8

Desjarlais M P, Kress J D and Collins L A 2002 *Phys. Rev.* E **66** 025401
Ehrenreich H and Philipp H R 1962 *Phys. Rev.* **128** 1622–9
El Ghemmaz A 1996 Contribution à l'étude des propiétés optiques des métaux liquides par ellipsometrie spectroscopique *PhD Thesis* Université de Metz
Faber T E 1972 *Introduction to the Theory of Liquid Metals* (London: Cambridge University Press)
Greenwood D A 1958 *Proc. Phys. Soc.* **71** 585–96
Jank W and Hafner J 1990 *Phys. Rev.* B **41** 1497–515
Junquera J, Paz Ó, Sánchez-Portal D and Artacho E 2001 *Phys. Rev.* B **64** 235111
Kaplow R, Strong S L and Averbach B L 1965 *Phys. Rev.* **138** A1336–45
Kresse G and Hafner J 1993 *Phys. Rev.* B **47** 558–61
Kubo R 1957 *J. Phys. Soc. Japan* **12** 570–86
Maksimov E G, Mazin I I, Rashkeev S N and Uspenski Y A 1988 *J. Phys. F: Met. Phys.* **18** 833–49
Mazin I I, Savitskii E M and Uspenski Y A 1984 *J. Phys. F: Met. Phys.* **14** 167–74
Nosé S 1991 *Prog. Theor. Phys. Suppl.* **103** 1–46
Ordejón P, Artacho E and Soler J M 1996 *Phys. Rev.* B **53** R10441–4
Read A J and Needs R J 1991 *Phys. Rev.* B **44** 13071–3
Recoules V, Clérouin J, Renaudin P, Noiret P and Zérah G 2003 *J. Phys. A: Math. Gen.* **36** 6033–9
Recoules V and Crocombette J P 2005 *Phys. Rev.* B **72** 104202
Recoules V, Renaudin P, Clérouin J, Noiret P and Zérah G 2002 *Phys. Rev.* E **66** 056412
Roll A and Motz H 1957 *Z. Metallk.* **48** 272–80
Schulz L 1957 *Adv. Phys.* **6** 102–44
Silvestrelli P L, Alavi A and Parrinello M 1997 *Phys. Rev.* B **55** 15515–22
Soler J M, Artacho E, Gale J D, García A, Junquera J, Ordejón P and Sánchez-Portal D 2002 *J. Phys.: Condens. Matter* **14** 2745–79
Troullier N and Martins J L 1991 *Phys. Rev.* B **43** 1993–2006
Tups H and Syassen K 1984 *J. Phys. F: Met. Phys.* **14** 2753–67
Uspenski Y A, Maksimov E G, Rashkeev S N and Mazin I I 1983 *Z. Phys.* **53** 263–70
Waseda Y 1980 *The Structure of Non-Crystalline Materials: Liquids and Amorphous Solids* (New York: McGraw-Hill)
Ziman J M 1961a *Adv. Phys.* **10** 1–56
Ziman J M 1961b *Phil. Mag.* **6** 1013–34